Dense Multipath Depolarization in Outdoor and Indoor Radio Transmissions

Enrico M. Vitucci[1], Francesco Mani[2], Vittorio Degli-Esposti[1] and Claude Oestges[3]

[1]University of Bologna, Dipartimento di Ingegneria dell'Energia Elettrica e dell'Informazione "Guglielmo Marconi" (DEI) Cesena, Italy – e-mail: v.degliesposti, enricomaria.vitucci @unibo.it

[2]Telecom ParisTech, COMELEC Department, Paris, France – e-mail: Francesco.Mani@telecom-paristech.fr

[3]Université catholique de Louvain, ICTEAM Electrical Engineering, Louvain-la-Neuve, Belgium – e-mail: claude.oestges@uclouvain.be

Abstract

The polarimetric properties of so-called Dense Multipath Components (DMC) are investigated in various outdoor and indoor environments, relying on broadband measurements and Ray-Tracing (RT) simulations. The ultimate goal is to parameterize a heuristic Diffuse Scattering model to be embedded in RT tools, in order to reproduce the experimentally observed cross-polar discrimination (XPD) characteristics.

1. Introduction

The depolarization of radio channels is of crucial interest when the polarization domain is exploited to leverage diversity or multiplexing gains in compact MIMO transmission schemes. In particular, the Cross Polarization Discrimination (XPD), usually defined as the ratio between the co-polarized and cross-polarized powers at the receiver, significantly impacts the performance of multi-polarized systems. However, the modeling of the polarimetric properties of the radio channel in general is quite challenging as the observable metrics usually result from the interaction of a number of mechanisms, including the antenna arrays. While traditional stochastic models account for global depolarization, they are still much too simple and cannot be easily scaled.

Prior experimental studies [1-7] show that cross-polarization coupling is low in rural areas, while it is higher in dense urban and indoor environments, where multipath richness is greater. The degree of directional spreading, especially in the elevation domain, appears to be a key factor for the determination of the depolarization [4, 6-7]. This calls for including in polarization models the so-called Dense (or Diffuse) Multipath Components, which are usually disregarded or over-simplified in radio channel models [4, 8].

Recent work has been carried out to develop a hybrid, deterministic-stochastic model called "Effective Roughness" (ER) model to include diffuse scattering in Ray Tracing (RT) models [4, 8-11], mostly focusing on outdoor scenarios. The present work, investigations are further extended to an indoor environment, where a multi-dimensional measurement campaign was previously performed using a MIMO channel sounder with dual-polarized antennas [12]. In the next section, the ER Diffuse Scattering model is briefly introduced and the measurement setup is described. Then the polarimetric characteristics of the DMC, and of the whole radio channel in general, are analyzed in detail and the ER model is parametrized in all the three cited environments.

2. Measurement-Based Parameterization of Dense Multipath Depolarization

2.1 Polarized Model of Diffuse Scattering

The polarimetric characterization of the DMC builds upon a diffuse scattering model based on the "Effective Roughness" approach [9-10]. For each wall-surface element, it is assumed that the impinging power is partially reflected specularly and partially scattered according to a given diffuse scattering coefficient *S*, which is the amount of power scattered in all the directions at the expense of the specular reflection. Several shapes of the scattering patterns are possible, but prior studies have revealed that a directive lobe centered on the direction of specular reflection provides the best fit to measured data [10-12],

$$A(\psi_R) = \left(\frac{1+\cos\psi_R}{2}\right)^{\alpha_R} \tag{1}$$

where ψ_R is the angle between the specular reflection direction and the scattering direction and α_R is an integer that sets the width of the scattering lobe. An additional parameter K_{xpol} is defined such that $1 \le K_{xpol} < 1$ to account for DMC depolarization [8, 11]. When K_{xpol} is equal to 0, the diffuse scattered field follows the polarization behavior of the specular field; when K_{xpol} increases, the cross-polarization coupling increases, and the scattered field reads as,

$$\mathbf{E}_s = \sqrt{1-K_{xpol}}\ \left|\mathbf{E}_S\right|\ e^{j\chi_1}\ \hat{i}_{co} + \sqrt{K_{xpol}}\ \left|\mathbf{E}_S\right|\ \hat{i}_{xp} \tag{2}$$

where unit vectors $\hat{i}_{co}$ describes the DMC polarization in the absence of depolarization, and $\hat{i}_{xp}$ is orthonormal to $\hat{i}_{co}$.

978-1-4673-5225-3/14/$31.00 ©2014 IEEE

2.2 Experimental Setups

In order to validate the model, measurements were performed in different types of outdoor and indoor environments with the UCL-ULB Elektrobit MIMO Channel Sounder, using a transmission bandwidth of 200 MHz. The carrier frequency was 3.8 GHz for the outdoor measurements, and 3.6 GHz for the indoor measurements. The transmit power was always 23 dBm. In the outdoor measurements, uniform linear arrays of four dual-polarized patch antennas (with +45°/-45° slanted polarization) were used at both transmit (Tx) and receive (Rx) sides. In the indoor measurements, the same linear array as in the outdoor measurements was used for the fixed terminal, while at the mobile terminal a tri-polarized antenna was used [12], which was moved with an automatic positioning device to create a virtual $5 \times 5 \times 5$ uniform cubic array. Three different categories of environments have been investigated to validate the model by means of measurements and RT simulations: two simple outdoor environments (isolated rural and office buildings), two complex urban environments (campus and street canyon) and two typical indoor environments (laboratory and office rooms). In each case, the following experimental setup has been used:

- isolated buildings: static measurements with Tx and Rx units facing the largest wall of the building under test; the Rx position is kept fixed, while the Tx unit is moved at different distances from the Rx unit;
- complex urban scenarios: dynamic measurements with a mobile pedestrian Tx and a fixed Rx unit (located on top of a building for the campus scenario and at pedestrian height in the canyon scenario);
- indoor environments: static measurements with the Rx unit being kept fixed in a room and the Tx unit being located at various positions along a route crossing different rooms [13].

Regarding the simulation setup, the diffuse scattering model has been embedded into a RT simulator, and its main parameters have been properly tuned to achieve a good agreement with the measurements in the different scenarios. Of course, also the polarimetric 3-D far field radiation patterns of all antenna elements of both Tx/Rx arrays, previously measured in anechoic chamber, have been input into the RT tool.

The polarimetric characteristics of the channel in the above mentioned scenarios, and in particular of the diffuse scattering component, are analyzed in the following using the cross-polar discrimination (XPD), that is defined as

$$XPD\ [dB] = 10\log_{10}\left(\frac{P_{co}}{P_{xp}}\right) \tag{3}$$

where P_{co} is the total narrowband power obtained with an integration of the channel impulse responses over all the co-polar channels. In a similar way, stands for the total cross-polar narrowband power.

2.3 Data Post-Processing and Modeling Results

Let us first consider the cases of two isolated buildings (one plain brick wall building and one typical urban office building). The DMC is eventually obtained after removing the line-of-sight (LOS) via a simple "time-gating" technique and the coherent paths (e.g. specular reflection) with the aid of RT simulation and SAGE [14-15] high-resolution algorithm (see [8] for further details). From the measured DMC, the diffuse component of (1) and (2) is parameterized. First, the values $S = 0.45$ and $S = 0.6$ are chosen for the rural and office building, respectively, while $\alpha_R = 2$ is assumed for both scenarios, as these values allow reproducing the same ratio between the DMC power and the total power found in the measurements, which is 29 % for the rural building, and 52 % for the office building [8]. The best value for K_{xpol} is then estimated. Table I outlines the average XPD values of DMC (data-based) and diffuse scattering (RT-based). It is worth noticing that introducing K_{xpol} is essential to achieve a good agreement between measured and simulated XPD levels. It is also interesting to compare the XPD of the coherent components (obtained from simulations) is equal to 12.2 and 10.4 dB, respectively for the rural and office buildings. This is quite high, but not surprising, since reflections and diffractions are not highly-depolarizing interactions. In the rural case, the total measured XPD is similar (10.8 dB), but in the office building scenario, the total measured XPD is as low as 5.4 dB. This is because DMC are much more significant and more depolarizing in the office building case, given to its much more complex façade.

Table I: Average XPD of Diffuse Scattering (measured and simulated)

Environment type	*XPD of DMC (measurements)*	*XPD of Diffuse Scattering (simulations, K_{xpol}=0)*	*XPD of Diffuse Scattering (simulations, best K_{xpol})*	*Best K_{xpol} value*
Rural building	9.57 dB	10.9 dB	8.73 dB	0.05
Office building	3.1 dB	8.54 dB	4.28 dB	0.2
Indoor office	0 dB	22.22 dB	0.19 dB	0.5
Indoor lab	-0.46 dB	23.02 dB	0.079 dB	0.55

Let us not extend the analysis to two large-scale built-up areas (a campus and a street canyon). Due to the complexity of the above mentioned scenarios and sounding limitations, it is not possible to extract the DMC from the measurements. Therefore, our analysis relies on the global XPD only, as summarized in Table II.

Table II: Average values of total XPD (measured and simulated) in the isolated building scenarios

Environment type	*Total XPD (measurements)*	*Total XPD (simulations, K_{xpol}=0)*	*Total XPD (simulations, best K_{xpol})*	*Best K_{xpol} value*
Campus	2.08 dB	4.41 dB	1.67 dB	0.3
Street canyon	0.67 dB	3.84 dB	1.51 dB	0.3

We first observe that the total XPD measured values are quite low, implying that the DMC and the coherent components contribute about equally to the cross-polarization coupling. This actually results from the absence of a strong line-of-sight: in the campus scenario, this is caused by a large distance between Tx and Rx, whereas the directional Tx and Rx patterns have not been facing each other in the street canyon. To parameterize the diffuse scattering model in the RT tool, we take S = 0.3 and S = 0.4, respectively, while α_R is chosen as 2 [11]. The best K_{xpol} value that guarantees a good agreement between the measured and simulated XPD values is estimated as 0.3 in both scenarios, which is significantly higher than the values found for isolated buildings.

As far as the indoor measurements are concerned, the use of a virtual antenna array at the mobile unit enables to separate the DMC from the specular multipath components using the SAGE high-resolution algorithm [14], as described in [12-13]. Additionally, this procedure allows de-embedding the antenna contribution, by contrast to the outdoor scenarios. As shown in Table II, the (antenna de-embedded) XPD of DMC is close to 0 dB in both measurement scenarios. This implies that in indoor environments, the DMC tends to fully depolarize the impinging wave. Taking S = 0.4 and α_R = 1 as recommended in [12] in the RT simulations, the best-fit K_{xpol} value is estimated as approximately 0.5, slightly higher than in the complex urban scenarios. By contrast, we also find that the total measured XPD is much higher (between 18 and 20 dB): this results from the presence of a dominant path (LOS or quasi-LOS), the power of which overshadows the DMC power.

Based on all reported evidence, we can draw the following conclusions regarding the impact of diffuse scattering on the amount of channel depolarization in a variety of environments:

- the depolarization degree of the DMC, modeled into the ER model through the parameter K_{xpol} appears to increase with the complexity of the environment,
- the DMC seems to play an important role in the determination of the actual degree of depolarization coupling in all cases, since the XPD of the DMC is always lower than the overall XPD,
- the overall depolarization level can be low – i.e. the XPD relatively high – even in complex environments such as indoors, mainly due to the low link distance and to the ubiquitous presence of a strong dominant path (LOS or obstructed-LOS) which overshadows the DMC contribution.

3. Application to Physical-Statistical Modeling of Façades

The full model integrating specular reflection and polarized diffuse scattering has been used in [15] to derive an physical-stochastic model of building façades in a land mobile satellite (LMS) context. Relying on RT simulations of an isolated building, each facade is represented (from the scattering viewpoint) as a cluster, shaped into a scattering disk aligned with the façade and whose center is located in the center of the real façade. Each scattering disk consists of a large number (typically, 15 to 20) point scatterers, each being assigned a given power and random phase. The scattering (including reflection) of an arbitrary facade is characterized by three parameters: the total scattered power density (per unit facade area), which enables to compute the total scattered power (to be divided between the individual point scatterers), the scattering cluster radius, which is related to the angular spread of the facade as seen by a receiver in the street, and the scattering depolarization. This simplified model enables to significantly decrease the simulation and to combine the façade modeling with existing geometry-based models of the LMS channel.

A typical simulation setup is described in Figure 1. It consists in a straight street lined with buildings of various heights on both sides. The satellite link is characterized by an azimuth of 90 degrees (i.e. orthogonal to the street axis) and an elevation of 60 degrees. The carrier frequency is taken as 1.6 GHz. The resulting narrowband received power is illustrated in Figure 2. The transition from line-of-sight to shadowed regions is clearly observed.

4. Acknowledgments

This work has been carried out in the framework of FP7 Network of Excellence NEWCOM# and COST Action IC1004. The application to physical-statistical modeling has been funded by the European Space Agency under ESA/ESTEC contract 4000104006/11.

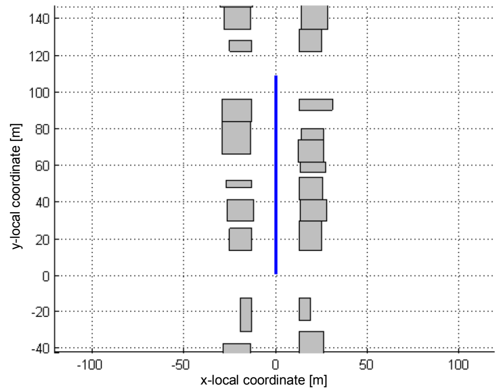

Figure 1 : Simulated street geometry and mobile trajectory

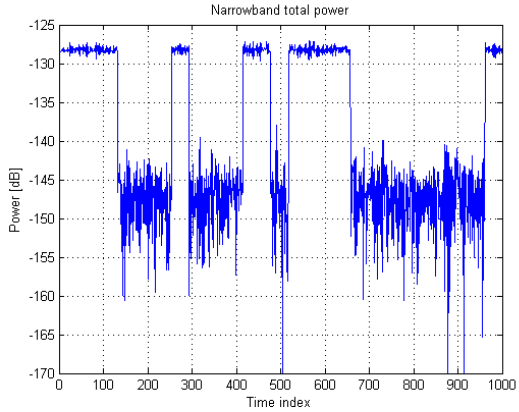

Figure 2 : Simulated received power along the street

5. References

1. H. Kuboyama, Y. Tanaka, K. Sato, K. Fujimoto, K. Hirasawa, "Experimental results with mobile antennas having cross-polarization components in urban and rural areas," *IEEE Transactions on Vehicular Technology*, Vol. 39, No. 2, May 1990, pp 150-160.
2. H. M. El-Sallabi, "Polarization consideration in characterizing radio wave propagation in urban microcellular channels," IEEE International Symposium on Personal, Indoor and Mobile Radio Communications, 2000, pp. 411-415
3. M. Landmann, K. Sivasondhivat, J.-I. Takada, I. Ida, and R. Thomae, "Polarization Behavior of Discrete Multipath and Diffuse Scattering in Urban Environments at 4.5 GHz," *EURASIP Journal on Wireless Communications and Networking*, 2007
4. V. Degli-Esposti, V.-M. Kolmonen, E. M. Vitucci, and P. Vainikainen, "Analysis and modeling on co- and cross-polarized urban radio propagation for dual-polarized MIMO wireless systems," *IEEE Transactions on Antennas and Propagation*, Vol.59, No.11, 2011, pp.4247-4256.
5. L. Vuokko, A. Kainulainen, P.Vainikainen, "Polarization behavior in different urban radio environments at 5.3 GHz," 8th International Symposium on Wireless Personal Multimedia Communications, Aalborg, Denmark, 2005, pp. 416-420.
6. M. Shafi, M. Zhang, A. L. Moustakas, P. J. Smith, A. F. Molisch, F. Tufvesson, and S. H. Simon, "Polarized MIMO Channels in 3-D: Models, Measurements and Mutual Information," *IEEE Journal on Selected Areas in Communications*, Vol. 24, No. 3, 2006, pp. 514-527.
7. L. E. Gurrieri , T. J. Willink , A. Petosa , S. Noghanian, "Characterization of the Angle, Delay and Polarization of Multipath Signals for Indoor Environments," *IEEE Trans. on Antennas and Propagation*, Vol. 56, No. 8, 2008, pp 2710-2719.
8. E. M. Vitucci, F. Mani, V. Degli-Esposti, and C. Oestges, "Polarimetric properties of diffuse scattering from building walls: Experimental parameterization of a ray-tracing model," *IEEE Transactions on Antennas and Propagation*, Vol. 60, No. 6, 2012, pp 2961-2969.
9. V. Degli-Esposti, "A diffuse scattering model for urban propagation prediction," *IEEE Transactions on Antennas and Propagation*, Vol. 49, No. 7, 2001, pp. 1111-1113.
10. V. Degli-Esposti, F. Fuschini, E. Vitucci, G. Falciasecca, "Measurement and modelling of scattering from buildings," *IEEE Transactions on Antennas and Propagation*, Vol. 55 No 1, 2007, pp. 143-153.
11. E. M. Vitucci, F. Mani, V. Degli-Esposti, and C. Oestges, "Study of a Polarimetric Model for Diffuse Scattering in Urban Environment," 6th European Conference on Antennas and Propagation, Prague, Czech Republic, 2012.
12. F. Mani, F. Quitin, and C. Oestges, "Directional spreads of dense multipath components in indoor environments: Experimental validation of a ray-tracing approach," *IEEE Transactions on Antennas and Propagation*, Vol. 60, No. 7, 2012, pp. 3389-3396.
13. F. Quitin, C. Oestges, F. Horlin, and P. De Doncker, "A polarized clustered channel model for indoor multi-antenna systems at 3.6 GHz," *IEEE Transactions on Vehicular Technology.*, Vol. 59, No. 8, 2010, pp. 3685-3693.
14. B. Fleury, P. Jourdan, and A. Stucki, "High-resolution channel parameter estimation for MIMO applications using the SAGE algorithm," *Int. Zurich Seminar Broadband Commun.*, 2002, pp. 301-309.
15. C. Oestges, N. Khan, F. Mani, and R. Prieto-Cerdeira, "A geometry-based physical-statistical model of land mobile satellite channels in urban environments, " 8th European Conference on Antennas and Propagation, The Hague, The Netherlands, 2014.